Thermal Performance of Crossflow Microchannel Heat Exchangers

Haishan Cao, Guangwen Chen,* and Quan Yuan

Dalian National Laboratory for Clean Energy, Dalian Institute of Chemical Physics, Chinese Academy of Sciences, Dalian 116023, People's Republic of China

Forced-convection heat transfer in a crossflow microchannel heat exchanger (MCHE) was investigated via experiment. The microchannels on the plates of the MCHE were machined using a chemical etching method from 0.4-mm-thick stainless steel plates, and the plates were bonded together by vacuum diffusion bonding. The influence of the aspect ratio of microchannels was analyzed based on MCHEs with two plates. The maximum volumetric heat-transfer coefficient using deionized (DI) water as the working fluid reached 11.1 MW m^{-3} K^{-1}, with a corresponding pressure drop of <6 kPa when the Reynolds number (*Re*) in the microchannels was ~64. Besides, the maximum volumetric heat-transfer coefficient, using air as the working fluid, was 0.67 MW m^{-3} K^{-1}, with a corresponding pressure drop of ~30 kPa when $Re \approx 1026$. Correlations of the average Nusselt number (*Nu*) and *Re* values were obtained from MCHEs with 2 plates, and their validity was confirmed by MCHEs with 2 and 10 plates.

1. Introduction

Metallic microstructure devices are increasingly applied in thermal and chemical process engineering, and the characteristics, advantages, and potentials of microstructure devices have been described in some references.[1−6] The microchannel heat exchanger (MCHE) is an essential microchemical engineering unit process device, which is suitable for many thermal and chemical processes with relatively large heat fluxes, such as electronic components colding,[7−9] turbine blade colding,[10] recovery of energy of miniature hydrogen production systems,[11] ammonia chiller,[12] etc.

However, relatively few definitive heat-transfer coefficients of MCHEs with different geometric structures and dimensions are offered in the published literature. Although intensive research investigating the laminar heat transfer in microchannels has been published over the past decades, most research was focused on fully developed regions in straight single microchannels. Moreover, some published results have significant differences, compared with the situation in large-scale channels. Wu et al.[13] reported that the Nusselt number (*Nu*) in laminar flow was closely related to the boundary conditions of heating surface of microchannels. Wang et al.[14] concluded that laminar heat transfer in microchannels was complicated, which was influenced by liquid temperature, velocity, and microchannel dimensions. Peng et al.[15] found that laminar heat transfer was dependent on the aspect ratio and the ratio of the hydraulic diameter to the center-to-center distance of microchannels. Possible reasons to interpret the discrepancies included surface roughness, variation of the predominate forces, surface electrostatic charges, axial heat conduction, measurement accuracy, etc.[16] Note that the effect of variation of predominate forces, surface electrostatic charges, and axial heat conduction were relatively small when the microchannel dimensions were more than a few hundred micrometers.

Harms et al.[17] investigated the convective heat transfer in rectangular microchannels ~1000 μm deep, with deionized (DI) water as the working fluid, through a single-channel system and a multiple-channel system. The widths of channels and channel walls in the multiple-channel system are 251 and 119 μm, respectively. Compared with the multiple -channel system, the unique difference in the single-channel system is the lack of channel walls. The results showed that the experimental *Nu* value for the single-channel system was higher than that predicted via classical relations presented by Shah and London (1978) and Gnielinski (1976), for laminar flow and turbulent flow, respectively. They considered this enhancement to be possibly caused by the effect of the inlet bend. The results for the multiple-channel system were consistent with classical relations at high flow rates, but deviated obviously at low rates. Harms et al. believed that this deviation was induced by flow bypass in the manifold. Nevertheless, they still felt that the classical relations are appropriate for designing microchannel systems under the condition of reasonable manifold design.

Unfortunately, for multiple-channel plates of different geometric structures, the degrees of inlet effect, fluid distribution, and channel roughness in channels exert different influences. In a previous study, our research group investigated the overall performance of counterflow MCHEs with multiple plates. The correlations of the average *Nu* value to the Reynolds number (*Re*) in microchannels were presented for designing MCHEs with multiple plates, and the validity of correlations was verified using MCHEs with 2 plates and 10 plates.[18] In the plates of counterflow MCHEs, the distribution chamber accounted for a relatively large area, which led to a smaller heat-transfer area. Besides, the pressure drop induced by the distribution chamber is relatively big. Based on these two points, the performance of crossflow MCHE was investigated.

2. Analysis

The heat-transfer coefficients on both hot and cold sides are an essential factor for designing MCHEs. The overall heat-transfer coefficient of MCHEs can be obtained using experimental data, by

$$U = \frac{Q_m}{A\Delta t_m F} \tag{1}$$

where Q_m is the heat-transfer rate between hot and cold fluids. Δt_m is the logarithmic mean temperature difference. A is the total heat-transfer area on one side of the plate. F is the

* To whom correspondence should be addressed. Tel.: +86 411 84379031. Fax: +86 411 84379327. E-mail address: gwchen@dicp.ac.cn.

10.1021/ie100107s
Published on Web 06/09/2010

correction factor for a cross-flow heat exchanger, which was discussed in detail by Smith[19] and Bowman et al.[20]

The relationship between the respective heat-transfer coefficients on the two sides and the overall heat-transfer coefficient was proposed by Wilson.[21] If the channels on the hot and cold sides have almost the same geometric structure, the Wilson plot method could be expressed as

$$\frac{1}{UA} = \frac{1}{h_h A} + \frac{\delta_w}{\lambda_w A} + \frac{1}{h_c A} \tag{2}$$

where λ_w and δ_w are the thermal conductivity of plate material and the thickness of partition wall, respectively. If the flow rate on the two sides can be almost equally controlled, it is reasonable to assume that the heat-transfer coefficient is the same on both sides; that is,

$$h_h = h_c = h = \frac{2}{(1/U) - (\delta_w/\lambda_w)} \tag{3}$$

The Nusselt number (Nu) is defined as

$$Nu = \frac{hD_h}{\lambda_f} \tag{4}$$

The volumetric heat-transfer coefficient could be expressed as

$$h_v = hB \tag{5}$$

where B is area density (the ratio of the total heat-transfer area on one side of the exchanger plate to the total volume of the plate).

Heat-exchanger effectiveness is defined as follows:

$$\varepsilon = \frac{\Delta t_{max}}{t_{h,i} - t_{c,i}} \tag{6}$$

where Δt_{max} is the maximum temperature difference for both sides.

For a single pass, crossflow heat exchanger with both fluids unmixed, the heat-exchanger effectiveness can be obtained via the number of transfer units (NTU) and C_r by the following formula:[22]

$$\varepsilon = 1 - \exp\left[\left(\frac{1}{C_r}\right)(\mathrm{NTU})^{0.22}\{\exp[-C_r(\mathrm{NTU})^{0.78}] - 1\}\right] \tag{7}$$

where C_r and NTU are defined by

$$C_r = \frac{(mc_p)_{min}}{(mc_p)_{max}} \tag{8}$$

$$\mathrm{NTU} = \frac{UA}{(mc_p)_{min}} \tag{9}$$

3. Experimental Apparatus and Procedure

Figure 1 shows a schematic diagram of the experimental apparatus used to test the performance of crossflow MCHEs using DI water as the cold fluid and air as the hot fluid. The test setup contains a pump, an electrical heater, a mass flow controller, a drying tube, an adjustment valve, an air compressor, an instrument to measure temperature, a personal computer (PC) data acquisition system, two water tanks, two filters, two differential-pressure transmitters, and an MCHE. The hot air was supplied via an air compressor to the MCHE after drying and heating. The cold water provided from one cold water tank flowed through the MCHE to the other cold water tank for recycling when the water recovered to ambient temperature. A similar experimental apparatus was adopted if the performance of crossflow MCHEs was investigated using DI water or air as the working fluid on both the hot and cold sides.

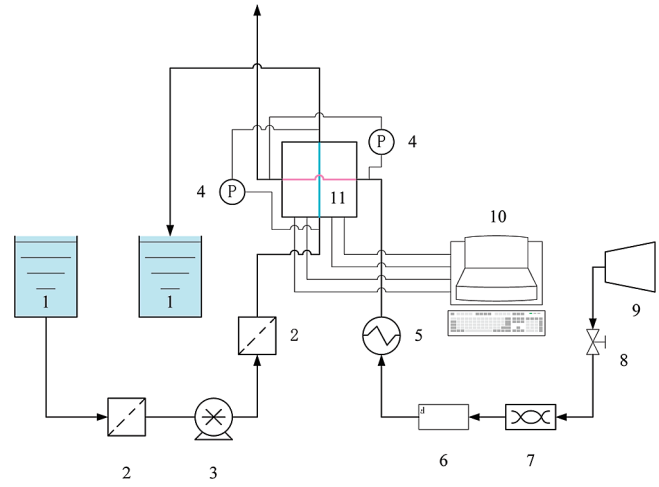

Figure 1. Schematic of the experimental apparatus. Legend: 1, water tank; 2, filter; 3, water pump; 4, differential-pressure transducer; 5, electric heater; 6, mass-flow controller; 7, drying tube; 8, adjustment valve; 9, air compressor; 10, multiplexer and computer; and 11, MCHE.

In this research, the plates of the MCHE were manufactured via a chemical etching method from 0.4-mm-thick stainless steel plates; the plates then were bonded via vacuum diffusion bonding. One exploded view of a crossflow MCHE and the geometric dimensions of the plate are presented in Figures 2 and 3, respectively. The detailed microchannel dimensions, channel number, and plate number of different type MCHEs are listed in Table 1. The surface roughness (R_a) of the plate was ~0.30 μm.

For each test, volumetric flow rates, pressure drops, and inlet and outlet fluid temperatures were measured at steady state. The flow rates of water and air were measured using the weighing method and a soap film gas meter, respectively. The maximum error in the flow rate was <1.6%. The pressure drops were measured using differential-pressure transmitters connected to digital display meters. The measurement uncertainty of differential pressure transmitters was within ±0.25 kPa. The temperatures are measured using Type T thermocouples, connected through a multiplexer to a PC. The multiplexer recorded the inlet and outlet temperatures of hot and cold fluids simultaneously every 2 s. Each measured temperature was usually the average of values recorded via the multiplexer within ~1 min. Temperature measurement errors were <1.0 K. Besides, the experimental errors in the heat balance were <5.0%.

To easily obtain the convection heat-transfer coefficients of different working fluids on both sides of the MCHE plate, the almost-equal volumetric flow rates of DI water or air were supplied to both passages of MCHEs with two plates. After that, the performance of the MCHE with 2 plates using DI water as the cold fluid and air as the hot fluid and the performance of the MCHE with 10 plates using DI water as both the cold fluid and the hot fluid were measured under the condition that the hot fluid flow rate was fixed and the cold fluid flow rate increased gradually. The purpose of the experiments is to verify that the convection heat-transfer coefficient obtained via MCHEs with 2 plates can be used to design MCHEs with multiple plates.

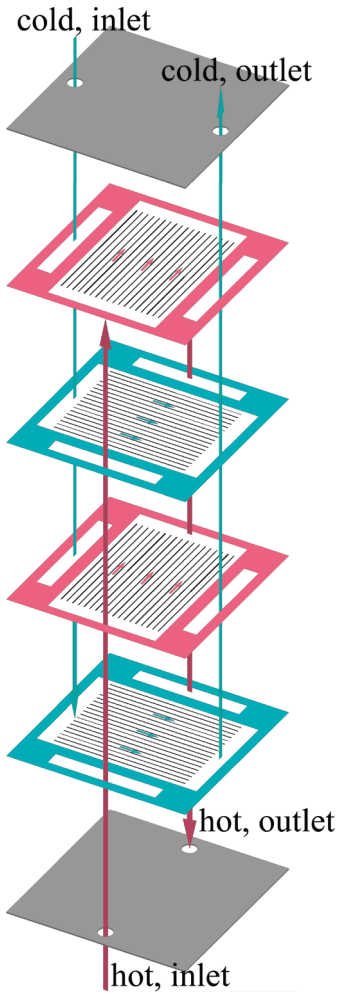

Figure 2. Exploded view of a crossflow MCHE with four plates.

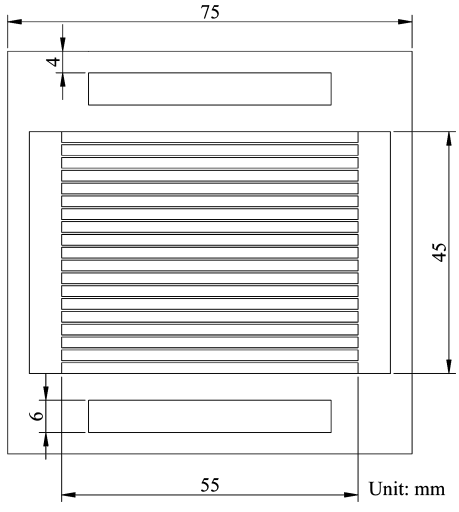

Figure 3. Geometric dimensions of a plate of the MCHE.

4. Results and Discussion

4.1. Performance of MCHEs Using Deionized Water as the Working Fluid. Figure 4 shows the volumetric heat-transfer coefficient in the MCHEs using DI water as the working fluid. The figure shows that the volumetric heat-transfer coefficient ascends dramatically as the *Re* value increases, when $Re < 20$. After that, the volumetric heat-transfer coefficient increases steadily as the *Re* value increases. The possible reason for this phenomenon is that the nonuniform fluid distribution in the plate seriously limits the normal performance of the MCHE when $Re < 20$. This suggests that the MCHEs do not bring their potential into full play when $Re < 20$. Moreover, we can see from the figure that the volumetric heat-transfer coefficient decreases as the channel width increases. The maximum volumetric heat-transfer coefficient arrives at 11.1 MW m^{-3} K^{-1} in MCHE 3 when $Re \approx 64$. When $Re > 20$, the maximum relative errors in the logarithmic mean temperature difference and the volumetric heat-transfer coefficient are 14.8% and 15.6%, respectively.

Table 1. Geometry Dimension of Crossflow MCHEs

	MCHE 1	MCHE 2	MCHE 2*	MCHE 3
number of plates	2	2	10	2
number of channels	19	32	32	49
channel length (mm)	55	55	55	55
channel width (μm)	2197	1194	1194	646
channel height (μm)	200	200	200	200
fin width (μm)	181	220	220	278
heat-transfer area (mm^2)	2203	2277	2277	2289
area density (m^2/m^3)	979	1012	1012	1017

Table 2. Performance of Microchannel Heat Exchanger (MCHE) Devices

reference	h_v (MW m^{-3} K^{-1})	Δp (kPa)	$h_v/\Delta p$ (kW m^{-3} K^{-1} Pa^{-1})
Cao et al.[18]	5.2	20	0.260
Jiang et al.[23]	38.4	70	0.548
Kang et al.[24]	188.5	2470	0.076
Hornung et al.[25]	34.7	3000−4000	0.008−0.012
experimental observations	11.1	6	1.85

Table 2 gives a comparison of the performance of MCHEs in this study, relative to that of microchannel heat exchanger devices investigated previously, using DI water as the working fluid.

To predict the heat-transfer performance of MCHEs with multiple plates via experimental data obtained from MCHEs with two plates, the relationship of the average *Nu* and *Re* values in the microchannels of the MCHE 1−MCHE 3 is shown in Figure 5, when $Re > 20$. According to the figure, the average *Nu* value increases as the *Re* value increases. The correlation of the average *Nu* value and the *Re* value in the microchannels of the MCHEs, which can be merged into one correlation gained by the least-squares fitting, is expressed as follows:

$$Nu = 1.72Re^{0.296} \tag{10}$$

Compared with one correlation of the average *Nu* value and the *Re* value gained through counterflow MCHE (eq 22 in ref 18), the average *Nu* value obtained from experimental data of

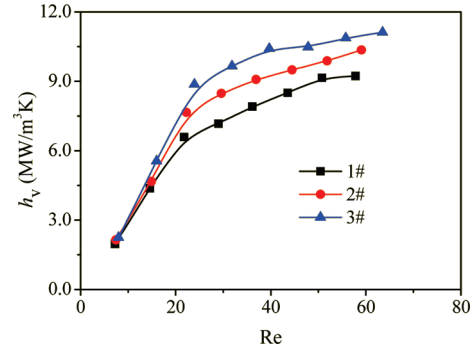

Figure 4. Volumetric heat-transfer coefficient in the MCHEs using DI water as the working fluid.

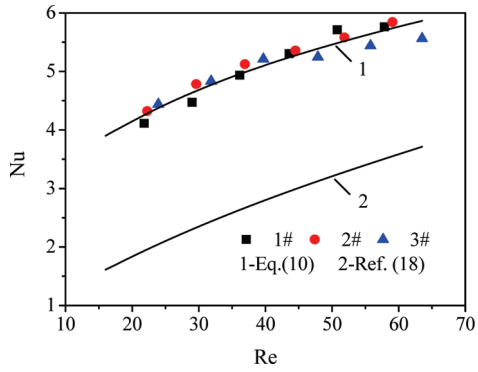

Figure 5. Average Nusselt number (*Nu*) as a function of the Reynolds number (*Re*) in microchannels for MCHEs, using DI water as the working fluid.

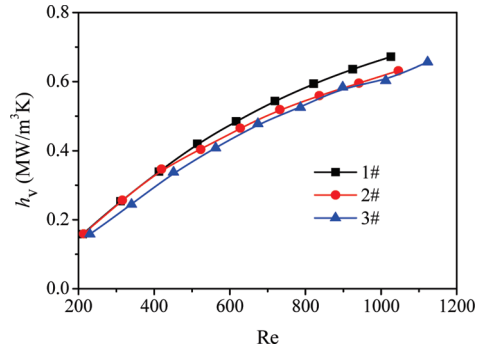

Figure 6. Volumetric heat-transfer coefficient in the MCHEs, using air as the working fluid.

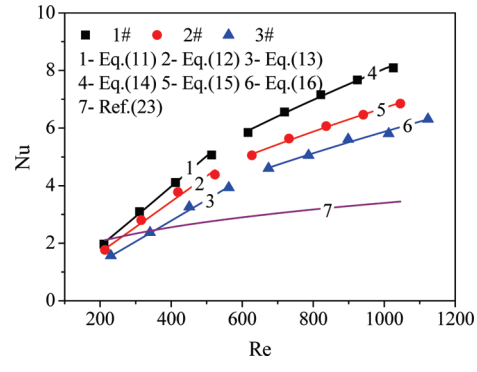

Figure 7. Average Nusselt number (*Nu*) as a function of the Reynolds number (*Re*) in microchannels for MCHEs, using air as the working fluid.

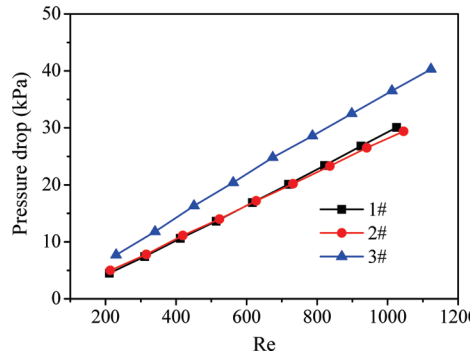

Figure 8. Pressure drop as a function of *Re* in the microchannels.

crossflow MCHE is obviously larger. One possible reason for this result is that the internal fluid distribution in the crossflow plate is better than that of counterflow plate.

Moreover, the maximum pressure drop of MCHEs investigated was <6 kPa when the *Re* value in the microchannels was ~64. This implies that full advantage of these types of MCHEs could be taken under higher volumetric flow rates and a larger volumetric heat-transfer coefficient could be obtained.

4.2. Performance of MCHEs Using Air as the Working Fluid. The volumetric heat-transfer coefficient in the MCHEs using air as the working fluid is shown in Figure 6. As shown in the figure, the volumetric heat-transfer coefficient increases gradually as the *Re* value increases. Besides, the influence of the dimensions of MCHEs on the volumetric heat-transfer coefficient is not as strong as the situation using DI water as the working fluid. To explain this phenomenon, it is necessary to mention the following points. First, the influence weight of the degree of uniformity of the internal fluid distribution in the plate on the volumetric heat-transfer coefficient may increase as the *Re* value increases. Second, as the *Re* value increases, the increasing length of the thermal developing region could weaken the influence of the dimensions of microchannels. Moreover, the maximum volumetric heat-transfer coefficient arrives at 0.67 MW m^{-3} K^{-1} in MCHE 1 at an *Re* value of 1026. Analysis shows that the maximum relative errors of logarithmic mean temperature difference and volumetric heat-transfer coefficient are 4.5% and 6.7%.

Figure 7 shows that the average *Nu* value increases as the *Re* value and the channel width each increase. Besides, the critical *Re* value lies between 520 and 680, and varies with channel width. Correlations of the average *Nu* value and the *Re* value in microchannels of MCHEs gained by the least-squares fitting are expressed as follows.

Re < 520:

$$Nu^{(1)} = 0.0068Re^{1.063} \quad (11)$$

$$Nu^{(2)} = 0.0072Re^{1.030} \quad (12)$$

$$Nu^{(3)} = 0.0053Re^{1.045} \quad (13)$$

Re > 680:

$$Nu^{(1)} = 0.0975Re^{0.639} \quad (14)$$

$$Nu^{(2)} = 0.1139Re^{0.590} \quad (15)$$

$$Nu^{(3)} = 0.0881Re^{0.608} \quad (16)$$

Compare these results with the correlation of average *Nu* and *Re* values introduced by Jiang et al.[23] According to the dimensions of MCHE 3, the average *Nu* value obtained from experimental data is obviously larger than the literature values when *Re* > 320.

The inconsistency of plates induced by chemical etching and diffusion bonding often causes a pressure drop discrepancy between the hot side and cold side, which are comprised of the same type plate. To truthfully reflect the influence of the dimensions of MCHEs as much as possible, the smaller pressure drop between both sides comprised of the same type plate is chosen to analyze the difference of pressure drops among plates of different types. As shown in Figure 8, the difference of pressure drops between MCHE 1 and MCHE 2 is small; however, the pressure drop in MCHE 3 is obviously higher than the two mentioned previously. The maximum pressure drop reaches 40.3 kPa in MCHE 3 at *Re* < 1123.

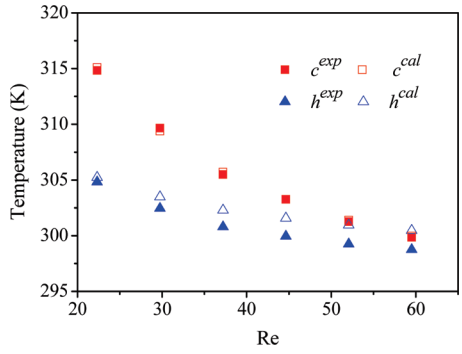

Figure 9. Experimental and predictive outlet temperature of MCHE 2.

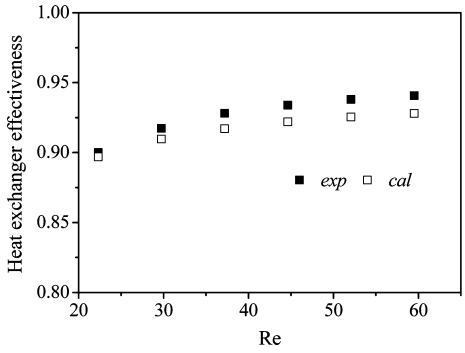

Figure 10. Experimental and predictive heat-exchanger effectiveness of MCHE 2.

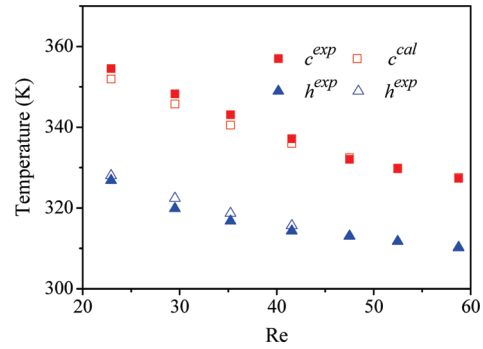

Figure 11. Experimental and predictive outlet temperatures of MCHE 2*.

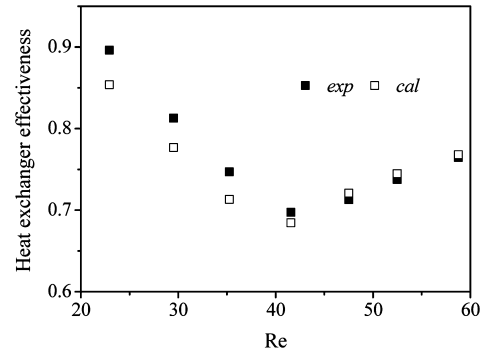

Figure 12. Experimental and predictive heat-exchanger effectiveness of MCHE 2*.

4.3. Performance Prediction. 4.3.1. Performance of MCHEs with Different Working Fluids. To verify the correlations of the average *Nu* value obtained, MCHEs with two plates can be used to design corresponding MCHEs; the performance of MCHE 2 was measured experimentally using air as the hot fluid with a fixed flow rate and DI water as the cold fluid with a varied flow rate.

Figure 9 shows that the predictive values of the outlet temperatures of MCHE 2 via eqs 10 and 15 agree with experimental values under the following conditions: a fixed hot air volumetric flow rate (20 L/min) and varied cold DI water volumetric flow rate (ranging from ~30 mL/min to 80 mL/min) and the maximum temperature difference of predictive and experimental values is ~1.7 K. Figure 10 shows the predictive and experimental heat exchanger effectiveness, which is dependent on eqs 7, 10, and 15. The heat-exchanger effectiveness exceeds 90% within this research scope and increases as the volumetric flow rate of cold DI water increases. The maximum heat-exchanger effectiveness difference between predictive and experimental values is only 1.2%. This means that the correlations of the average *Nu* value obtained can be used to design corresponding MCHEs.

4.3.2. Scale-up Performance of MCHE. To further prove the correlations can be used to design corresponding MCHEs with multiple plates, the performance of MCHE 2* was investigated using DI water as the working fluid of two streams.

Figure 11 indicates that the predictive results of outlet temperatures of MCHE 2* via eq 10 are consistent with experimental results, under the following conditions: fixed hot fluid volumetric flow rate (265 mL/min) and varied cold fluid volumetric flow rate (ranging from ~154 mL/min to 395 mL/min). The difference between the experimental value and the predictive value decreases as the fluid flow rate increases, and the maximum temperature difference value is ~2.5 K when the corresponding cold fluid flow rate reaches its lowest point. This suggests that the performance of MCHEs with multiple plates can be effectively predicted through the correlations obtained from experimental data. Besides, the outlet temperatures of the experimental values of the cold fluid and the predictive values of the hot fluid are, respectively, higher than corresponding predictive values and experimental values in the region of relatively low volumetric flow rate. The reason for this may be that the fluid distribution in MCHE 2* is improved, compared with that of MCHEs with two plates in this region. This implies that the fluid distribution in MCHE with multiple plates is better than that of MCHEs with two plates if the mean volumetric flow rate is the same in the each plate.

Figure 12 shows the heat-exchanger effectiveness of MCHE 2* via experiment and prediction, depending on eqs 7 and 10; the difference is relatively large in the region of relatively low volumetric flow rate. Besides, the real values of heat-exchanger effectiveness of MCHE 2* are better than that of the predictive values. This also indicates the fluid distribution in MCHE with multiple plates is better. Moreover, the heat-exchanger effectiveness, ranging from ~0.7 to 0.9, decreases initially as the volumetric flow rate increases and reaches the bottom when the cold fluid volumetric flow rate is almost equal to the fixed hot fluid volumetric flow rate and then increases as the volumetric flow rate increases.

5. Conclusion

The fluid flow and forced convectional heat-transfer performance of crossflow microchannel heat exchangers (MCHEs) were investigated via experimental methods. The thermal performance of crossflow MCHEs with two plates, using deionized (DI) water as the working fluid, was successfully tested with Reynolds number (*Re*) values in microchannels of <70; the corresponding volumetric heat-transfer coefficient increases as *Re* increases but decreases as the channel width

increases. The maximum volumetric heat-transfer coefficient reached 11.1 MW m^{-3} K^{-1}. Besides, the thermal performance of crossflow MCHEs with two plates, using air as the working fluid, was investigated with the *Re* value in the microchannels ranging from 200 to 1200, and the corresponding volumetric heat-transfer coefficient increases with the increasing Reynolds number. However, the influence of channel width to volumetric heat-transfer coefficient is not strong. The maximum volumetric heat-transfer coefficient is 0.67 MW m^{-3} K^{-1}. Moreover, the performance of crossflow MCHE with 2 plates, using DI water as the cold fluid and air as the hot fluid, and crossflow MCHE with 10 plates using DI water as the working fluid, was successfully predicted via the correlations obtained from experimental data of crossflow MCHEs with 2 plates.

Acknowledgment

We gratefully acknowledge the financial support of the Ministry of Science and Technology of China (Nos. (2006AA020101, 2007AA030206 and 2009CB219903) and Fund of Dalian Institute of Chemical Physics, CAS (No. K2009D01) for this work.

Nomenclature

A = heat-transfer area (m^2)
B = area density (m^2/m^3)
c_p = specific heat (J kg^{-1} K^{-1})
C_r = ratio of heat capacity
D_h = hydraulic diameter of the channel (m)
F = heat-exchanger correction factor
h = heat-transfer coefficient (W m^{-2} K^{-1})
U = overall heat-transfer coefficient (W m^{-2} K^{-1})
h_v = volumetric heat-transfer coefficient (W m^{-3} K^{-1})
m = mass-flow rate (kg/s)
Nu = Nusselt number
Δp = pressure drop (kPa)
Q = heat-transfer rate (W)
Re = Reynolds number
R_a = arithmetical mean deviation of the profile
T = temperature (K)
Δt_m = logarithmic mean temperature difference (K)
Δt_{max} = maximum temperature difference for both sides (K)

Greek Symbols

δ = wall thickness (m)
λ = thermal conductivity (W m^{-1} K^{-1})
ε = heat-exchanger effectiveness

Subscripts

c = cold fluid
cal = calculated results
exp = experimental results
f = fluid
h = hot fluid
i = inlet
m = mean
o = outlet
w = wall

Literature Cited

(1) Schubert, K.; Brandner, J.; Fichtner, M.; Linder, G.; Schygulla, U.; Wenka, A. Microstructure devices for applications in thermal and chemical process engineering. *Microscale Thermophys. Eng.* **2001**, *5*, 17–39.

(2) Brandner, J. J.; Bohn, L.; Henning, T.; Schygulla, U.; Schuberth, K. Microsructure heat exchanger applications in laboratory and industry. *Heat Transfer Eng.* **2007**, *28*, 761–771.

(3) Chen, G. W.; Li, S. H.; Yuan, Q. Pd-Zn/Cu-Zn-Al catalysts prepared for methanol oxidation reforming in microchannel reactors. *Catal. Today* **2007**, *120*, 63–70.

(4) Chen, G. W.; Li, S. H.; Li, H. Q.; Jiao, F. J.; Yuan, Q. Methanol oxidation reforming over a $ZnO-Cr_2O_3/CeO_2-ZrO_2/Al_2O_3$ catalyst in a monolithic reactor. *Catal. Today* **2007**, *125*, 97–102.

(5) Ge, H.; Chen, G. W.; Yuan, Q.; Li, H. Q. Gas phase partial oxidation of toluene over modified V_2O_5/TiO_2 catalysts in a microreactor. *Chem. Eng. J.* **2007**, *127*, 39–46.

(6) Fan, Y. L.; Luo, L. A. Recent Applications of Advances in Microchannel Heat Exchangers and Multi-Scale Design Optimization. *Heat Transfer Eng.* **2008**, *29*, 461–474.

(7) Fedorov, A. G.; Viskanta, R. Three-dimensional conjugate heat transfer in the microchannel heat sink for electronic packaging. *Int. J. Heat Mass Transfer* **2000**, *43*, 399–415.

(8) Zhao, C. Y.; Lu, T. J. Analysis of microchannel heat sinks, for electronics colding. *Int. J. Heat Mass Transfer* **2002**, *45*, 4857–4869.

(9) Nika, P.; Bailly, Y.; Jeannot, J. C.; De Labachelerie, M. An integrated pulse tube refrigeration device with micro exchangers: Design and experiments. *Int. J. Therm. Sci.* **2003**, *42*, 1029–1045.

(10) Marques, C.; Kelly, K. W. Fabrication and performance of a pin fin micro heat exchanger. *J. Heat Transfer* **2004**, *126*, 434–444.

(11) Delsman, E. R.; De Croon, M. H. J. M.; Pierik, A.; Kramer, G. J.; Cobden, P. D.; Hofmann, C.; Cominos, V.; Schouten, J. C. Design and operation of a preferential oxidation microdevice for a portable fuel processor. *Chem. Eng. Sci.* **2004**, *59*, 4795–4802.

(12) Hrnjak, P.; Litch, A. D. Microchannel heat exchangers for charge minimization in air-cooled ammonia condensers and chillers. *Int. J. Refrig.* **2008**, *31*, 658–668.

(13) Wu, P. Y.; Little, W. A. Measurement of the heat-transfer characteristics of gas-flow in fine channel heat-exchanger used for micro-miniature refrigerators. *Cryogenics* **1984**, *24*, 415–420.

(14) Wang, B. X.; Peng, X. F. Experimental investigation on liquid forced-convection heat-transfer through microchannels. *Int. J. Heat Mass Transfer* **1994**, *37*, 73–82.

(15) Peng, X. F.; Peterson, G. P. Convective heat transfer and flow friction for water flow in microchannel structures. *Int. J. Heat Mass Transfer* **1996**, *39*, 2599–2608.

(16) Guo, Z. Y.; Li, Z. X. Size effect on microscale single-phase flow and heat transfer. *Int. J. Heat Mass Transfer* **2003**, *46*, 149–159.

(17) Harms, T. M.; Kazmierczak, M. J.; Gerner, F. M. Developing convective heat transfer in deep rectangular microchannels. *Int. J. Heat Fluid Flow* **1999**, *20*, 149–157.

(18) Cao, H. S.; Chen, G. W.; Yuan, Q. Testing and Design of a Microchannel Heat Exchanger with Multiple Plates. *Ind. Eng. Chem. Res.* **2009**, *48*, 4535–4541.

(19) Smith, D. M. Mean Temperature Difference in Cross-Flow. *Engineering.* **1934**, *2*, 479–481.

(20) Bowman, R. A.; Mueller, A. C.; Nagee, W. M. Mean Temperature Difference in Design. *Trans. ASME* **1940**, *62*, 283–294.

(21) Wilson, E. E. A Basis for Rational Design of Heat Transfer Apparatus. *Trans. ASME* **1915**, *37*, 47–82.

(22) Incropera, F. P.; DeWitt, D. P.; Bergman, T. L.; Lavine, A. S. *Fundamentals of Heat and Mass Transfer*, 6th ed.; Wiley: Singapore, 2006; p 389.

(23) Jiang, P. X.; Fan, M. H.; Si, G. S.; Ren, Z. P. Thermal-hydraulic performance of small scale micro-channel and porous-media heat-exchangers. *Int. J. Heat Mass Transfer* **2001**, *44*, 1039–1051.

(24) Kang, S. W.; Chen, Y. T.; Chang, G. S. The Manufacture and Test of (110) Orientated Silicon Based Micro Heat Exchanger. *Tamkang J. Sci. Eng.* **2002**, *5*, 129–136.

(25) Hornung, C. H.; Hallmark, B.; Hesketh, R. P.; Mackley, M. R. The fluid flow and heat transfer performance of thermoplastic microcapillary films. *J. Micromech. Microeng.* **2006**, *16*, 434–447.

Received for review June 20, 2009
Revised manuscript received April 5, 2010
Accepted May 25, 2010

IE100107S